



## Research article

## Synthesis and characterization of polystyrene with embedded silver nanoparticle nanofibers to utilize as antibacterial and wound healing biomaterial

Mayar Mostafa<sup>a</sup>, Nadia G. Kandile<sup>a</sup>, Mahmoud K. Mahmoud<sup>b</sup>, Hassan M. Ibrahim<sup>c,\*</sup><sup>a</sup> Chemistry Department, Faculty of Women for Arts, Science and Education, Ain Shams University, Heliopolis, 11757, Cairo, Egypt<sup>b</sup> Housing and Building National Research Center, 87 El Tahrir St., Dokki, Giza, 1770, Egypt<sup>c</sup> Textile Research and Technology Institute, National Research Centre, 33 El Bohouth St. (Former El Tahrir St.) P.O.12622, Dokki, Giza, Egypt

## ARTICLE INFO

## Keywords:

Wound healing  
Biomaterials antibacterial polystyrene nanofibers  
Silver nanoparticles

## ABSTRACT

Herein, silver nanoparticles (Ag) embedded in polystyrene (PS) nanofiber composites have been prepared by an electrospinning technique using N, N-dimethylformamide (DMF) as a solvent and safe reducing agent. Electrospinning of polystyrene (PS) solutions is conducted using different electrospinning parameters such as polymer concentration in the electrospinning solution; solution feed rate, and electrical field strength. Then silver nanoparticles (AgNPs) were embedded into PS nanofibers to obtain an AgNPs-PS nanofiber composite as a powerful, cheap, and nontoxic bioactive material. PS nanofibers and AgNPs-PS nanofibers composite were characterized by using thermogravimetric analysis (TGA), X-ray diffraction, and scanning electron microscopy (SEM). Also, AgNPs were characterized by UV-vis spectroscopy, transmission electron microscopy (TEM), and EDX analysis. Results showed that PS nanofibers were obtained with concentrations ranging from 10–30 wt.% in DMF solvent. Also, an AgNPs-PS nanofiber composite has been produced from its solutions by using DMF at the optimum value. The prepared AgNPs have a 21–40 nm particle size and a semi-spherical shape. In addition, the antibacterial activity of AgNPs-PS nanofibers towards both Gram-positive and Gram-negative bacteria has been increased. Therefore, this nanocomposite can be used as a powerful bioactive material in biomedical fields.

## 1. Introduction

Nanotechnology has grown rapidly in recent decades because it can control particle size to fit functions that would otherwise be impossible to fit using conventional methods [1, 2]. Chronic wounds, such as foot ulcers in diabetics, cannot heal in simple progress and remain open or partially healed for a longer time than usual [3]. These types of wounds can be contaminated with a bacterial infection. Therefore, polymeric nanofibers as a developed wound dressing can be used to enhance wound healing performance instead of conventional wound dressing because they can promote hemostasis, fluid absorption, gas permeation, and cell respiration [4, 5].

Polystyrene (PS) represents one of the most useful and cheap thermoplastic polymers because it is transparent, colorless, and a brilliant material [6, 7]. In addition, it has high heat and electrical resistance with lower dielectric loss and is lightweight. These distinct properties make it widely used in several application fields, such as transparent material for

food packaging, electric covers, insulators, lamp covers, filters, and thermal comfort breathable textiles [8, 9, 10]. Polystyrene applications are limited due to their brittleness and poor mechanical properties [11, 12]. Therefore, many improvements to PS materials have been made, such as blending with other polymers and a new process for PS fabrication to produce PS materials with high mechanical and chemical properties [1, 13, 14].

The electrospinning process is simple, cheap, and easy. So, it has been used as an efficient method to produce ultra-fine nanofibers [15, 16]. These nanofibers have excellent properties such as extra-large surface to volume ratio, small fiber diameters, porous surface, and more functional surface [17, 18, 19, 20, 21, 22, 23]. Therefore, they can be applied in several fields, such as filters, wound dressing, protective clothes, medical fields, sensors, drug delivery, tissue engineering, cosmetics, and biomedical fields [4, 10, 16, 24, 25, 26, 27, 28, 29].

The electrospinning process produces continuous filament from a polymer solution under a high-voltage electric field. Then these filaments

\* Corresponding author.

E-mail address: [hmaibrahim@gmail.com](mailto:hmaibrahim@gmail.com) (H.M. Ibrahim).

**Table 1.** Experimental design of electrospinning of polystyrene solution.

Parameters	Levels
Concentration, wt.%	10, 15, 20, 25 and 30
Extrusion Rate, ml/h	1, 2 and 3
Field, kV/cm	2 and 3
<b>Total Runs</b>	<b>5 × 3 × 2 = 30</b>

are deposited on the collector. This process depends on several factors such as viscosity, surface tension, and solution conductivity [30, 31, 32].

Most electrospun nanofibers are accompanied by bead formation. Enton explains that these beads' formation results from the jet instability of a polymer solution [33, 34, 35]. Whereas Reneker reported that the bead formation results from both solution viscosity and surface tension net charge density from the electrospinning process. So based on these explanations it can be concluded that polymer with low concentration preferred bead formation and polymer with high concentration preferred fiber formation [6, 27, 36, 37].

Electrospun nanofibers can be applied in several fields, such as water-oil separation, ion exchanger, tissue engineering, enzyme immobilization, and sensors [4, 10]. The produced PS nanofibers have high mechanical properties with different morphology and are superhydrophobic material [24].

The morphology of electrospun PS nanofibers play an important role in the final product that is used in a specific application, therefore there are more essential to produce beads-free PS nanofibers [10, 11]. Many parameters must be studied to obtain PS uniform nanofibers based on polymer properties (molecular weight, concentration, viscosity, conductivity, surface tension, and solvent used) [11, 15, 24, 38].

Solvent type plays an important role in PS fiber morphology. Therefore, many solvents were studied for the electrospinning of PS, such as 1,2-dichloroethane, N, N-dimethylformamide (DMF), ethyl acetate, methyl ethyl ketone (MEK), and tetrahydrofuran (THF) [10, 11, 39]. From these solvents, DMF was the most favourite solvent to produce uniform PS nanofibers with a smooth surface due to its higher boiling point, conductivity, and dielectric constant compared to other solvents [10, 24].

Several studies reported that metal nanoparticles could be incorporated within nanofibers to impart antibacterial activity to be used in biomedical applications [40, 41]. Among these metal nanoparticles, silver nanoparticles (AgNPs) have been widely used as a bioactive polymeric material, due to their catalytic activity, higher conductivity,

antibacterial activity, and nontoxic nature [42, 43, 44]. Therefore, AgNPs incorporated into PS nanofibers can find more applications, especially for filtration, food packaging, and medical textiles [41, 45, 46]. AgNPs have been widely used as antibacterial materials because they are nontoxic to humans [4, 47, 48].

A stable and colloidal dispersion of AgNPs was prepared through chemical reduction methods by using borohydride and hydrazine as reducing agents [36, 38, 49]. Although these reducing agents have higher activity, they cause environmental toxicity that limits their applications [44, 50]. Thus, using a nontoxic reducing agent such as N, N-dimethylformamide (DMF) can present an eco-friendly way to prepare safe silver nanoparticles (AgNPs). Therefore, DMF can be introduced as a nontoxic reducing and solvent medium agent (stabilizer or capping agent) for AgNPs impregnated PS nanofiber composite [15, 16, 51].

In the present work, PS and AgNPs-PS nanofibers composite were prepared from N, N-dimethylformamide (DMF) as a solvent and reducing agent via an electrospinning process. Different electrospinning parameters were studied. The prepared nanofibers were characterized by FT-IR, TGA, XRD, UV-Vis, TEM, SEM, and EDX analysis. The antibacterial activity of AgNPs-PS nanofibers was evaluated towards *S. aureus* and *E. coli* via the disc inhibition zone.

## 2. Materials and methods

### 2.1. Materials

Sigma-Aldrich, USA, provided analytical grade polystyrene with Mw of 20, 200, and 2000 kDa. Dimethylformamide (DMF) was purchased from Merck Chemicals, Germany. Silver nitrate was purchased from Fisher Scientific. Polystyrene was used for the initial trials with dimethylformamide (DMF) as the solvent. These trials were conducted to confirm the trials carried out by previous researchers.

### 2.2. Methods

#### 2.2.1. Preparation of polystyrene electrospinning solution

The desired amount of polystyrene, according to the concentration required, was weighed. Polystyrene was poured into a glass bottle containing dimethylformamide. The glass bottle has to be closed with an airtight lid to maintain the concentration throughout. A homogeneous solution was achieved by slow agitation. This was either by keeping the

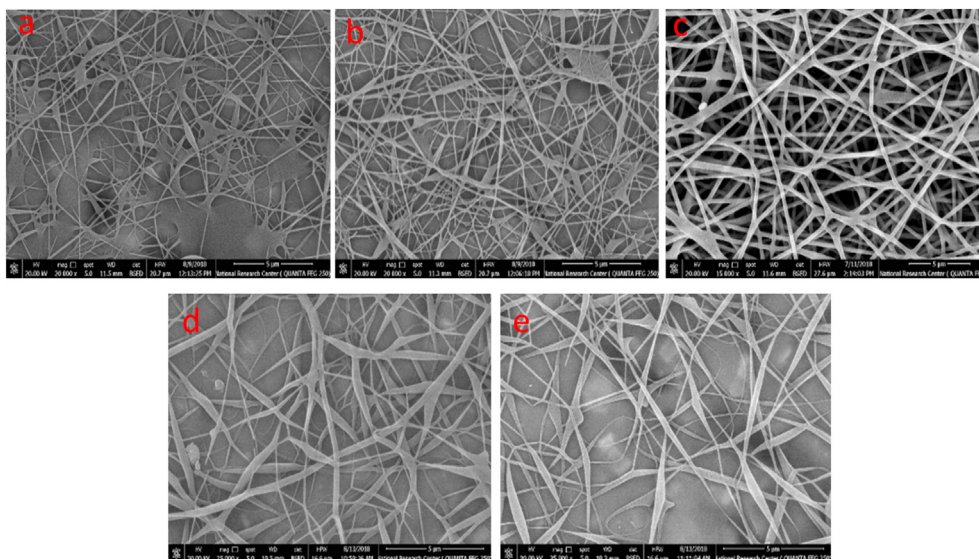


**Figure 1.** SEM images of Polystyrene nanofibers samples at 10 wt.% (a), 15 wt.% (b), 20 wt.% (c), 25 wt.%, and 30 wt.% concentrations (e) at a 1 ml/h extrusion rate and a 3 kV/cm field.

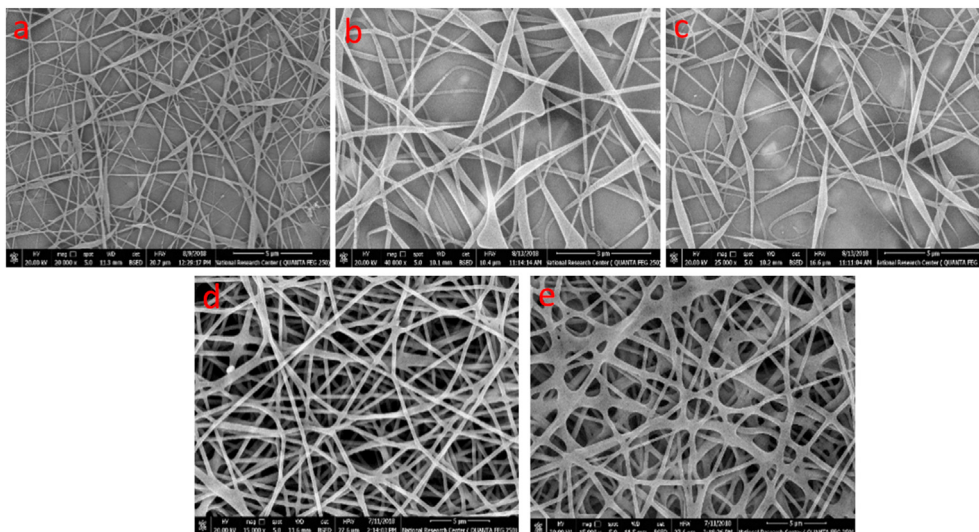


**Figure 2.** SEM Images of Polystyrene nanofibers samples of 10 wt. % (a), 15 wt. % (b), 20 wt. % (c), 25 wt. % and 30 wt. % concentration (e) at an Extrusion Rate of 1 ml/h and Field of 2 kV/cm.

solution for some time or by using a magnetic stirrer. The agitation was slow to avoid mechanical degradation of the polymer chains. All solutions were prepared at room temperature. The solution is kept overnight so that a homogeneous solution can be obtained.

### 2.2.2. Preparation of PS solution containing silver nanoparticles (AgNPs)

It was carried out as follows: A 15% wt.% PS solution was prepared in DMF solvent by stirring the mixture overnight. Thereafter, AgNO<sub>3</sub> (1% wt.% calculated based on the weight of PS) was added into the solution, which was kept overnight in the dark and then the solution was refluxed for 1 h to reduce AgNO<sub>3</sub>. The solution became dark yellow because of the formation of AgNPs [9].

### 2.2.3. Electrospinning of polystyrene solution

Electrospinning was used to create an electrospun polystyrene (PS) nanofiber and an AgNPs embedded PS nanofiber composite. Appropriate solutions were transferred into a syringe equipped with a needle, and the fiber was collected on an aluminium collecting plate. The operation process of this system can be carried out by switching on the power of the high voltage system and slowly increasing the voltage

through a regulator, which starts at 0 kV and is kept constant at 30 kV during the electrospinning process. The polymer solutions are sprayed towards the collector. The amount of polymer in the solution was based on the desired basis weight. A layer of nanofibers was produced on the aluminium foil with a dimension of 30 cm × 30 cm. The 14th piece of aluminium foil was partially covered with gauze fabric (possibly as part of wound dressing). This allowed the formation of two samples for each run. One sample was on the top of the aluminium foil and the other was on the gauze fabric. The sample on the aluminium foil was used for SEM images to characterize the structure, and the sample on the gauze was used to determine the antibacterial properties. The gauze's fairly open structure did not cause any problems with electrical field weakening, and the fibers spun on the top of the gauze were not different from the fibers spun directly over the aluminium foil.

### 2.2.4. Experimental design of electrospinning of polystyrene

Initial trials of electrospinning of polystyrene showed that nanofibers were formed at concentrations of 10–30 wt.% of polystyrene solution, whereas other concentrations below 5% produced films and

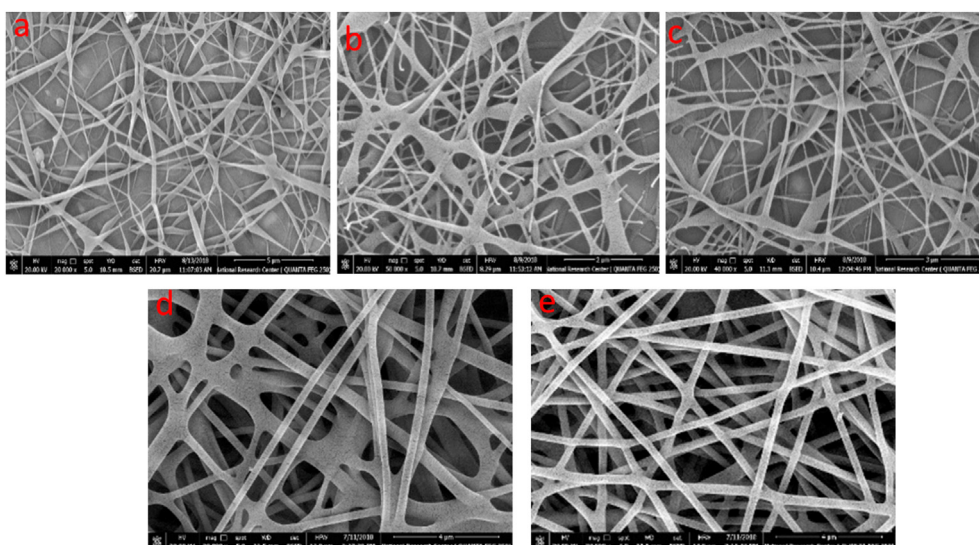


**Figure 3.** SEM images of Polystyrene nanofibers samples at 10 wt. % (a), 15 wt. % (b), 20 wt. % (c), 25 wt. %, and 30 wt. % concentrations (e) at a 2 ml/h extrusion rate and a 3 kV/cm field.



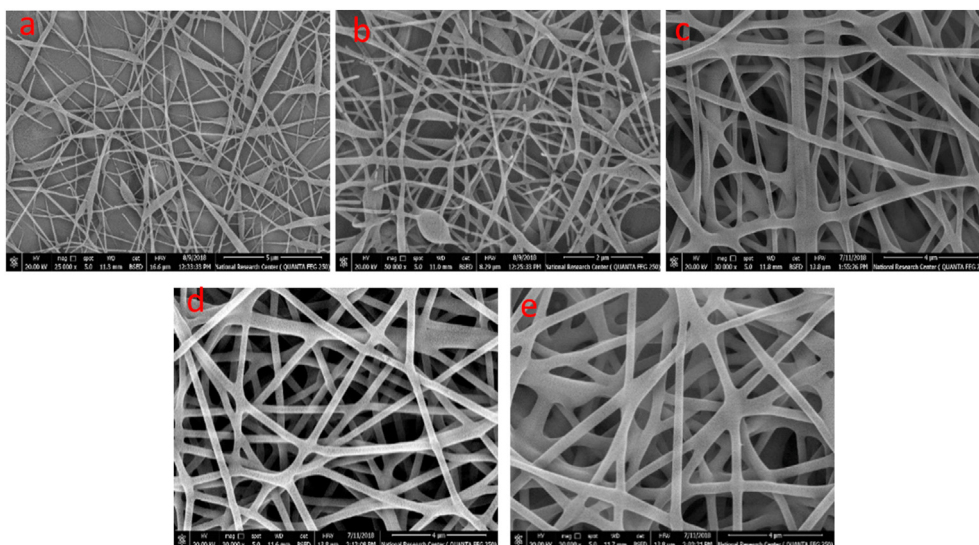


**Figure 4.** SEM images of Polystyrene nanofibers samples at 10 wt.% (a), 15 wt.% (b), 20 wt.% (c), 25 wt.%, and 30 wt.% concentrations (e) at a 2 ml/h extrusion rate and a 2 kV/cm field.

beads. To obtain the exact conditions for the electrospinning of polystyrene, different experimental designs were developed. Table 1 shows the dependent parameters and their levels for experimental design.

In this experimental design, basis weight ( $8.92 \text{ g/m}^2$ ) and voltage (25 kV) were kept constant, and the field was changed by varying the distance between the drum surface and the tip of the needle.

### 2.3. Characterization

#### 2.3.1. Transmission electron microscope (TEM)

Transmission electron microscopy (TEM) and a JEOL JEM 2100 F electron microscope at 200 kV were used to examine the morphology and particle size of AgNPs.

#### 2.3.2. X-ray diffraction (XRD)

Studies were conducted using an X-ray diffractometer (D2 Phaser, Bruker AXS, Germany) operating at 30 kV and 10 mA. The diffraction patterns were recorded using Cu-K radiation, and the film samples were analyzed at a  $2\theta$  degree range from 1–50.

#### 2.3.3. Scanning electron microscope (SEM) and energy dispersive X-ray spectroscopy (EDX)

A Scanning electron microscope (SEM) and an energy-dispersive X-ray spectroscope (EDX) for selected polystyrene nanofibers and their embedded AgNPs were used to record the morphology changes, the electrospun nanofiber diameter, and the elemental composition of the nanofiber surface. Quanta TM 250 FEG (Field Emission Gun) with a 30 kV accelerating voltage, FEI Co., Netherlands, was used for SEM and EDX analysis.

#### 2.3.4. Thermogravimetric analysis (TGA)

Thermogravimetric analysis (TGA) was performed at a temperature starting from  $25^\circ\text{C}$  to  $600^\circ\text{C}$  under an inert nitrogen atmosphere with a heating rate of  $10^\circ\text{C min}^{-1}$  using the instrument: SDT Q600 V20.9 Build 20, USA.

#### 2.3.5. Surface tension and viscosity

Surface tension was measured using a Fisher Tensiomat. The viscosity of the solution at different concentrations was measured with a Brookfield viscometer.

**Table 2.** Polystyrene nanofibers at different parameters: concentration, extrusion rate, and high voltage field.

	Sample No.	Concentration, %	Morphology	Fiber Diameter, nm*
Extrusion Rate 1 ml/h and Field 3 Kv/cm	1	10	Beads + Fibers	$96 \pm 6.64$
	2	15	Fibers + Beads	$167 \pm 11.55$
	3	20	Fibers	$278 \pm 19.23$
	4	25	Fibers	$292 \pm 20.19$
	5	30	Fibers	$329 \pm 22.76$
Extrusion Rate 1 ml/h and Field 2 Kv/cm	6	10	Fibers + Beads	$72 \pm 5.02$
	7	15	Fibers + Beads	$168 \pm 11.62$
	8	20	Fibers	$278 \pm 19.25$
	9	25	Fibers	$329 \pm 22.77$
	10	30	Fibers	$459 \pm 31.79$
Extrusion Rate 2 ml/h and Field 3 Kv/cm	11	10	Beads + Fibers	$63 \pm 4.38$
	12	15	Fibers + Beads	$175 \pm 12.11$
	13	20	FibBeads + Fibers	$208 \pm 14.43$
	14	25	Fibers	$243 \pm 16.86$
	15	30	Fibers	$486 \pm 33.65$
Extrusion Rate 2 ml/h and Field 2 Kv/cm	16	10	Fibers + Beads	$67 \pm 4.66$
	17	15	Fibers + Beads	$123 \pm 8.57$
	18	20	Fibers	$222 \pm 15.38$
	19	25	Fibers	$380 \pm 26.30$
	20	30	Fibers	$483 \pm 33.42$
Extrusion Rate 3 ml/h and Field 3 kv/cm	21	10	Fibers + Beads	$55 \pm 3.87$
	22	15	Fibers + Beads	$178 \pm 12.38$
	23	20	Fibers	$208 \pm 14.43$
	24	25	Fibers	$358 \pm 24.80$
	25	30	Fibers	$456 \pm 31.55$
Extrusion Rate 3 ml/h and Field 2 Kv/cm	26	10	Fibers + Beads	$71 \pm 4.95$
	27	15	Fibers + Beads	$132 \pm 9.19$
	28	20	Fibers	$250 \pm 17.31$
	29	25	Fibers	$369 \pm 25.54$
	30	30	Fibers	$471 \pm 32.64$

(\*) For n = 100 readings, data are expressed as mean S.D.

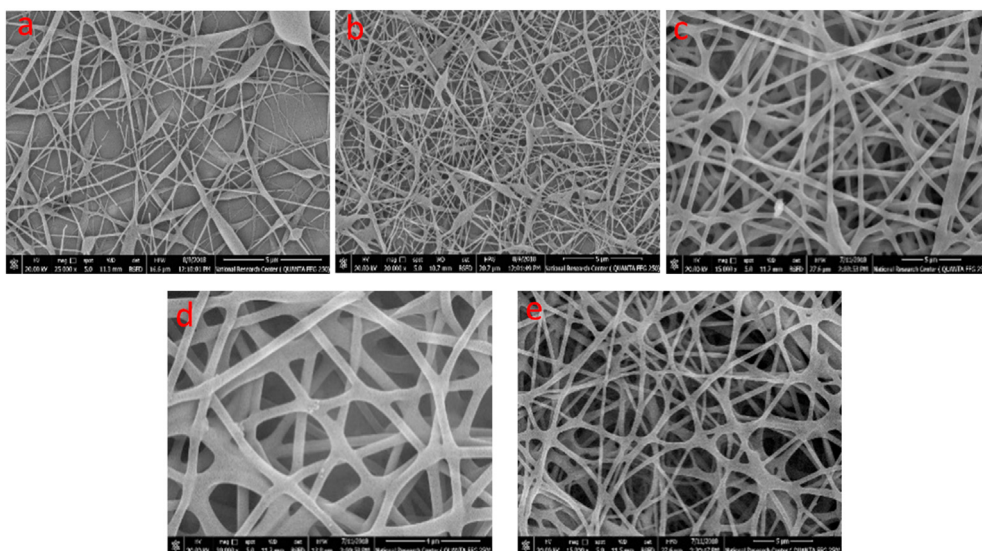


**Figure 5.** SEM images of Polystyrene nanofibers samples at 10 wt.% (a), 15 wt.% (b), 20 wt.% (c), 25 wt.%, and 30 wt.% concentrations (e) at a 3 ml/h extrusion rate and a 3 kV/cm field.

## 2.4. Evaluation of antibacterial activity via disk diffusion method

### 2.4.1. Materials

Two bacterial strains were provided by the Faculty of Women for Art, Science, and Education, Ain Shams University, and Cairo, Egypt. They include *E. coli* (ATCC 11229) and *S. aureus* (ATCC 6538). These strains were chosen because they are the most common bacteria found in wound infections. Fresh inoculants for antibacterial assessment were prepared in nutrient broth at 37 °C for 24 h.

### 2.4.2. Test method

The antibacterial activity of the prepared nanofibers was determined by the disc diffusion method on an agar plate as described in the previous work [16, 32]. In the antibacterial assay, all the data were the means of at least three parallel experiments, and the discrepancies among them were less than 5%.

## 2.5. Statistical analysis

Results were expressed as the mean value with its standard deviation (mean  $\pm$  S.D.) of each sample that was repeated three times ( $n = 3$ ). Statistical analysis was performed with the student's t-test and differences were considered significant at p-values below 0.05.

## 3. Results and discussion

### 3.1. Electrospinning of polystyrene solution

Initial trials were conducted with regard to the electrospinnability of polystyrene polymer. This was a necessary step to reveal the range of parameters that provide nanofibers. In an attempt to find the upper limit of the concentration parameter, the polystyrene was dissolved in dimethylformamide (DMF) at 35 wt.% and 40 wt.% concentrations. Due to the

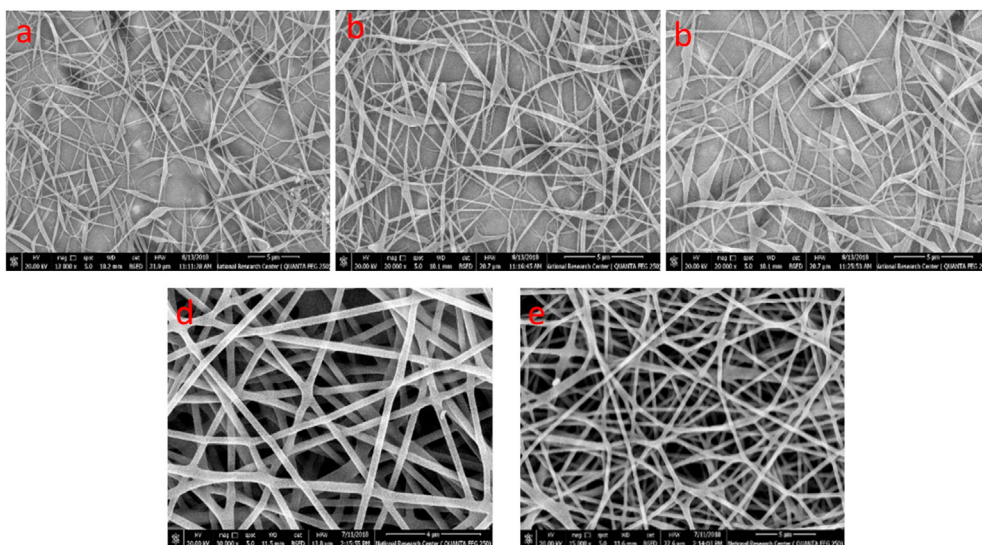


**Figure 6.** SEM images of Polystyrene nanofibers samples at 10 wt.% (a), 15 wt.% (b), 20 wt.% (c), 25 wt.%, and 30 wt.% concentrations (e) at a 3 ml/h extrusion rate and a 2 kV/cm field.

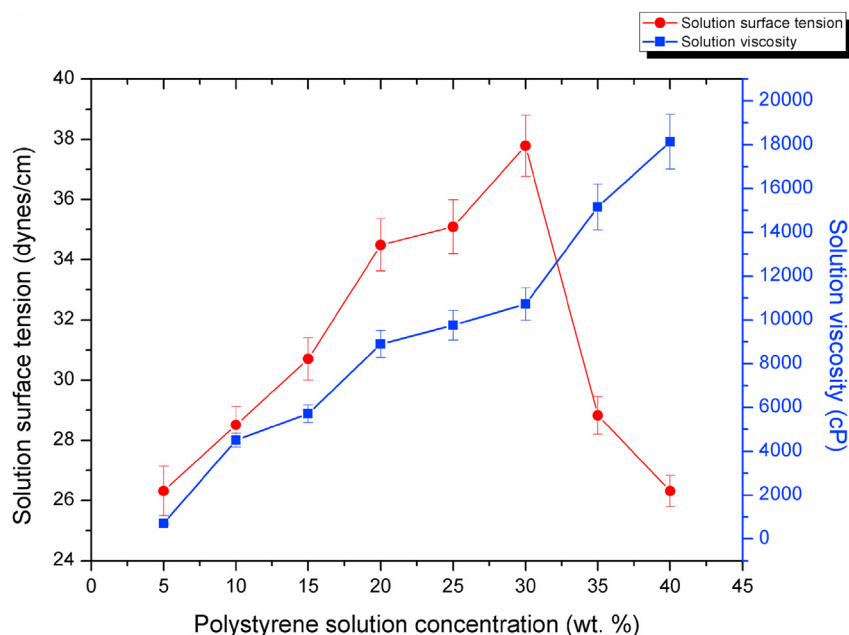


Figure 7. Surface tension and viscosity of polystyrene solution at different concentrations.

**Table 3.** The effect of AgNPs weight percent (wt.%) on atomic absorption and antibacterial activity of AgNPs embedded in PS nanofiber composites.

AgNPs wt.%	Atomic Absorption (mg/L)	Inhibition zone, mm	
		<i>S. aureus</i>	<i>E. coli</i>
without	0.000	00	00
0.031	67	5.0	00
0.25	114	11	4.0
0.75	148	12	7.0
1.00	235	17	12
1.25	378	21	16

All of these measurements were made with a polystyrene solution containing 15% weight of polystyrene (15 g PS in 100 ml of distilled water).

high viscosity, it was impossible to pump the solution through the spinneret at these two high concentrations. A stronger pumping power system and/or larger spinneret size may be needed to overcome such difficulties. The highest spinnable solution concentration was found to be 30%. The distance between the collection surface (drum) and the spinneret was maintained at 10 cm with an applied voltage of 25 kV. To find out the lower limit of spinnable solution concentration, different solutions were prepared with a range of concentrations of 5–40 wt.%. Electrospinning trials were conducted from these solutions and the corresponding SEM images are shown. Initial trials were conducted with regard to the electrospinnability of polystyrene polymer. This was a necessary step to reveal the range of parameters that provide nanofibers. In an attempt to find the upper limit of the concentration parameter, the polystyrene was dissolved in dimethylformamide (DMF) at 35 wt.% and 40 wt.% concentrations. Due to the high viscosity, it was impossible to pump the solution through the spinneret at these two high concentrations. A stronger pumping power system and/or larger spinneret size may be needed to overcome such difficulties. The highest spinnable solution concentration was found to be 30%. The distance between the collection surface (drum) and the spinneret was maintained at 10 cm with an applied voltage of 25 kV. To find out the lower limit of spinnable solution concentration, different solutions were prepared with a range of concentrations of 5–40 wt.%. Electrospinning trials were conducted from

these solutions and the corresponding SEM images are shown in Figures 1, 2, 3, 4, 5, 6.

At low polymer concentrations of 5–8%, beads and discontinuous films were formed. At such a low level of concentration, the solutions do not contain sufficient material to produce stable, solid continuous fibers. With increasing polymer concentration, the number of direct interchain associations of polystyrene molecules in the solution increases and reaches a critical value for forming a three-dimensional network structure (highly viscous gel), thereby forming a good spinnable solution. But as the concentration was increased to 10 %, 15%, 20%, 25%, and 30%, continuous fibers were formed.

Table 2 Depicts the effect of processing parameters of electrospinning of polystyrene on fiber diameter for the thirty samples along with the electrospinning process and solution parameters.

### 3.1.1. Electrospun polystyrene solution characterization

The electrospinning of polystyrene solutions depends on various factors, such as surface tension and viscosity. Beyond a certain surface tension, the Taylor cone breaks into the jets, which get deposited onto the collector plate as nanofibers. As viscosity increases, surface tension reduces.

As previously stated, the surface tension of the solution is associated with the formation of beads and beaded fibres at constant electrospinning parameters. The surface tension of the polymer solution was measured at different concentrations to obtain the most suitable polystyrene concentration having the suitable surface tension to form nanofibers.

The results of surface tension are shown in Figure 7, where the surface tension of polystyrene solutions decreased as their viscosity increased. As the viscosity increased, the solute-solvent interaction within the polymer also increased at high voltage during electrospinning. The solvent molecules will be spread over the entangled polymer molecules. Table 3 shows that as the concentration of polystyrene solution increased from 5% to 40%, the surface tension reduced and the most suitable values of surface tension were 28.60 and 37.90 dyn/cm for electrospinning of polystyrene.

Figure 7 shows that the viscosity of polystyrene solution increased as its concentrations increased. This was accompanied by the formation of



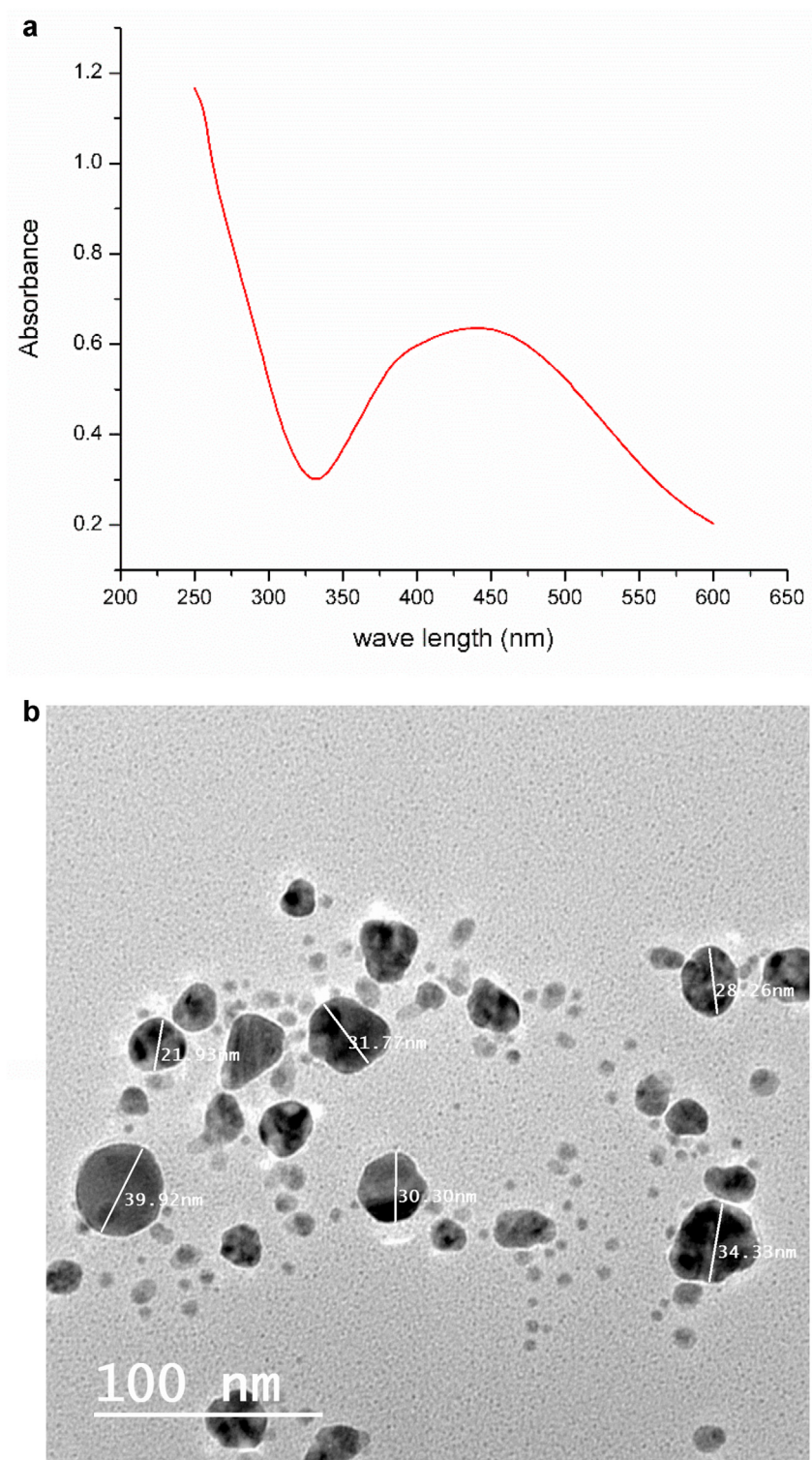


**Figure 8.** a. UV-Vis spectra of silver nanoparticles (AgNPs) prepared by DMF reduction method. b. TEM image of silver nanoparticles (AgNPs).

nanofibers at higher viscosity. This was because there was a greater amount of PS polymer available at higher concentrations. This was caused by more intermolecular attachments, which finally led to fiber formation. During initial trials of electrospinning using solutions of 5% and 8% concentration, there was no sufficient amount of polymer to form the fibers that resulted in the formation of beads and films. As the concentration increased, the viscosity and the amount of polymer in the solution increased, which in turn increased the fiber-forming property of

the solution. Thus, the excellent viscosity of the solution of polystyrene in DMF was found in a range of 4521–10757 cP.

### 3.2. Electrospinning of AgNPs embedded in polystyrene (PS) nanofiber composites as antibacterial nanofibers

The preparation method of the AgNPs embedded PS nanofibers composite by using electrospinning has been illustrated as follows:

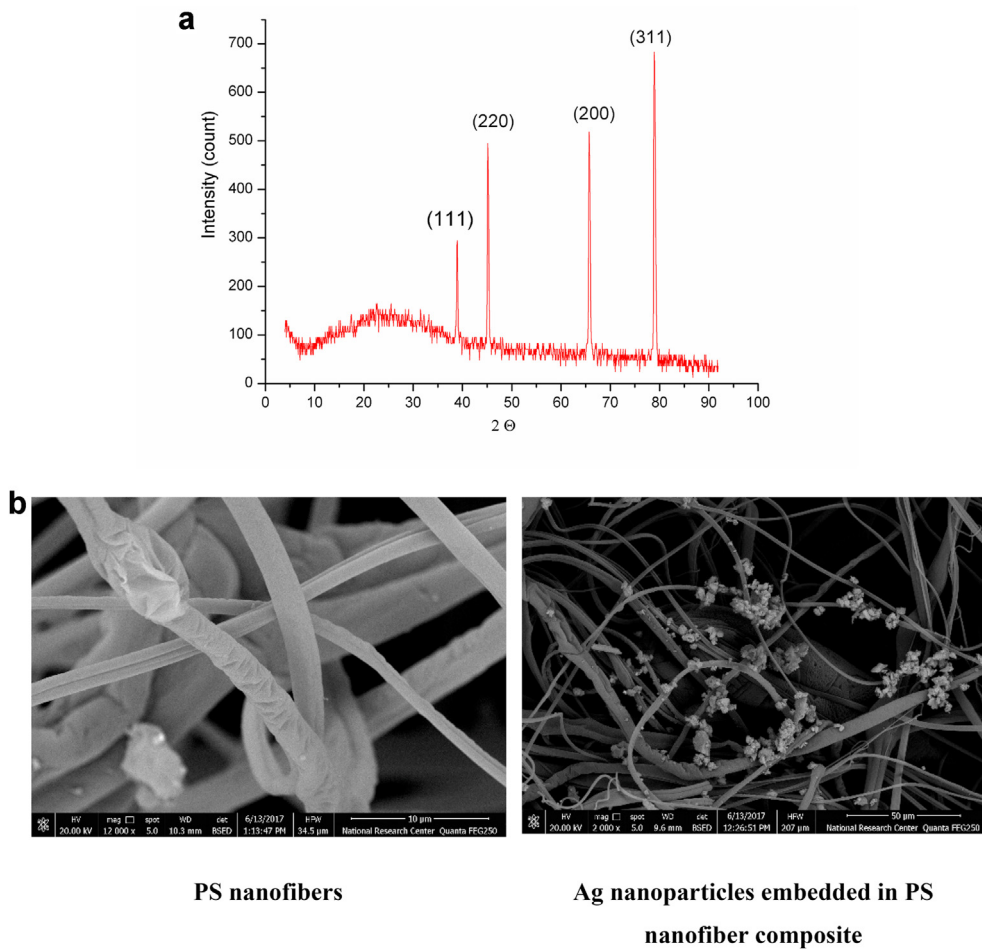


Figure 9. a. XRD pattern of AgNPs embedded PS nanofibers composite. b. SEM images of PS nanofibers and Ag nanoparticles embedded in PS nanofiber composite.

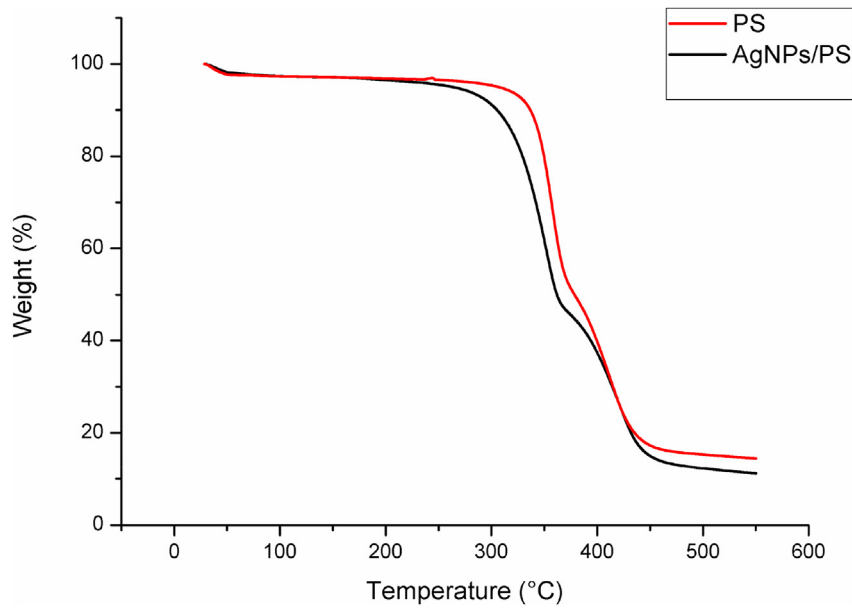


Figure 10. PS nanofiber and Ag NPs embedded in PS nanofiber composite TGA thermogram.



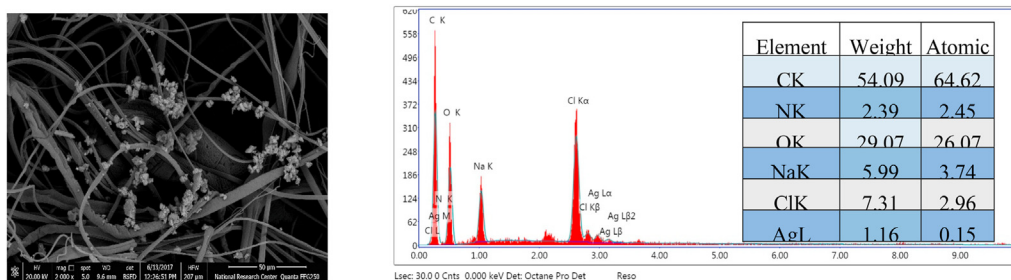
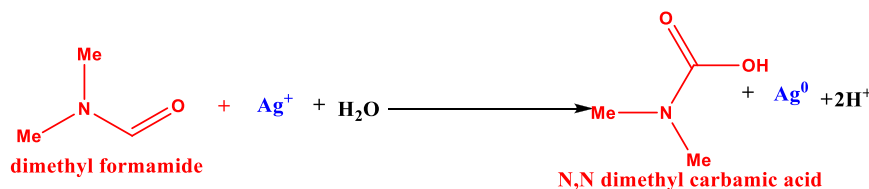


Figure 11. SEM and EDX analysis of AgNPs embedded PS nanofibers composite.

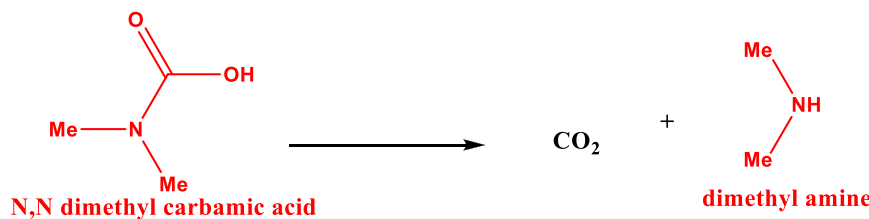
PS–DMF (15 wt.%) + AgNO<sub>3</sub> solution (1 wt.%)  $\xrightarrow[2. \text{ electrospinning process}]{1. \text{ reflux for } 1 \text{ h}}$  AgNO<sub>3</sub>  
– PS nanofibers composite

### 3.2.1. The mechanism of AgNO<sub>3</sub> reduction in DMF

N, N-dimethylformamide can be oxidized in the presence of silver nitrate to form carbamic acid and Ag<sup>+</sup> reduced to AgNPs as follows:



Then carbamic acid can be easily decomposed at T > 250 K into dimethylamine and carbon dioxide as follows.



Therefore, DMF has been used as a solvent for electrospinning of polystyrene solutions, and besides, it can also act as a self-reducing agent for the reduction of Ag ions [52], and the reflux process can increase the rate of reaction (conversion of silver ions to silver nanoparticles). The formation of a yellowish-brown colour after refluxing confirmed the reduction of Ag<sup>+</sup> ions and the subsequent formation of metallic Ag nuclei as AgNPs [16].

Figure 8a shows the UV-Vis. spectra of AgNPs-PS nanofibers prepared by the DMF reduction method. The observed UV-Vis spectrum at a wavelength in the range of 400–450 nm confirmed the formation of Ag nanoparticles after reflux with N, N dimethylformamide (DMF).

The TEM images of Ag nanoparticles are presented in Figure 9a. The diameters of the Ag nanoparticles varied from 21 to 40 nm. The nanoparticles of Ag are seen in the TEM images, and some of them are aggregated.

The presence of Ag nanoparticles within nanofibers was confirmed by XRD (Figure 9a) of the produced AgNPs-PS nanofiber composite. The XRD pattern showed 2θ values at 39.1, 46.1, 68.7, and 79.2, which could be indexed to four reflections from the (111), (200), (220), and (311) planes. The peaks in XRD suggest that Ag nanoparticles have a cubic

structure [53]. The size of silver nanoparticles within the nanofiber composite was about 19 nm.

The SEM images of PS nanofibers and Ag nanoparticles embedded in PS nanofibers composite were shown in Figure 9b.

The thermal stability of polystyrene nanofibers (PS) and silver nanoparticles embedded in polystyrene nanofibers composite (AgNPs-PS) were studied by using thermogravimetric (TGA). TGA of PS and

AgNPs-PS nanofiber composite are shown in Figure 10.

PS nanofiber demonstrated more thermal stability compared to the

AgNPs-PS nanofiber composite, with decomposition rates of PS from 368 to 455 °C, T<sub>max</sub>. at 419 °C, and half temperature at 417 °C with no residue material after burning. For AgNPs embedded in PS nanofibers composite, these data have been shifted to 356–449 °C (decomposition temperature), a 412 °C maximum temperature with a 406 °C half temperature, and 13% material residue after burning. This could be because of the catalytic effect of Ag nanoparticles on the thermal degradation of the Ag NPs/PS composite.

Figure 11 shows Scanning electron microscopy analysis (SEM/EDS) that confirmed the presence of AgNPs within the polystyrene (PS) electrospun nanofibers. In addition, silver nanoparticles (AgNPs) were deposited on the surface of PS electrospun nanofibers on a smooth surface. Therefore, SEM images showed the presence of small nanoparticles formed in a homogeneously distributed outside the nanofiber composite. In addition, EDX analysis confirmed that these formed nanoparticles were AgNO<sub>3</sub>. Furthermore, EDX analysis revealed that the Ag content was 1.16 wt.% [54].

Atomic absorption was another tool used to confirm the presence of Ag nanoparticles within the polystyrene nanofiber composite, as shown in Table 3. Therefore, atomic absorption has been successfully used to

determine the exact amount of AgNPs present on the PS nanofiber composite.

### 3.2.1. Evaluation of the antibacterial activity of AgNPs embedded in PS nanofibers composite

**3.2.1.1. Mechanism of antibacterial activity of AgNPs.** There are several mechanisms that have been described for the antibacterial activity of AgNPs. AgNPs carrying positive charges can attach to bacterial cell membranes carrying negative charges that enhance AgNPs' antibacterial effect [55]. AgNPs could attach to the bacterial cell wall membrane, then it penetrates the cell wall of bacteria and disturbs bacterial cellular contents. Reactive oxygen species (ROS) or oxidative stress is formed, causing bacterial death [56]. AgNPs can disrupt protein and phosphorus inside the bacterial cell and destabilize ribosome and DNA functions [57]. AgNPs can interfere with the respiratory chain and cell division, which leads to cell death [58].

The disc inhibition zone method was used to investigate the antibacterial activity of PS nanofibers and AgNPs/PS nanofibers composite against *S. aureus* and *E. coli* as Gram-positive and Gram-negative bacteria. Table 3 showed that PS nanofibers didn't inhibit bacterial growth while AgNPs/PS nanofibers composite inhibited bacterial growth due to the presence of AgNPs on the PS nanofibers. The antibacterial activity of the AgNPs-PS nanofiber composite was increased as the amount of AgNPs increased. This was due to enhancement of the electrostatic interaction between AgNPs and negative charges on the bacterial cell [56].

## 4. Conclusion

At the same time, nanofibers from PS and AgNPs-PS composites were successfully prepared from DMF as a solvent and reducing agent at the same time. PS nanofibers were formed at concentrations ranging from 10–30 wt.%, with a PS concentration of 20%, an extrusion rate of 1 ml/h, and a field of 3 kV/cm producing the best results. The optimum values of surface tension of PS were 28.60 and 37.90 dyn/cm and excellent values of viscosity in a range of 4521–10757 cP. Ag nanoparticles can be prepared by using DMF as a reducing agent and have a diameter of 21–40 nm. XRD and EDX analysis confirmed the presence of Ag nanoparticles within nanofibers. TGA confirmed that the thermal stability of PS nanofiber was greater than that of the PS-AgNPs nanofiber composite. EDX and SEM imaging confirmed the presence of AgNPs on PS nanofibers. Antibacterial activity results of the AgNPs-PS nanofibers composite against *S. aureus* and *E. coli* were increased due to the presence of AgNPs. Based on these results, AgNPs-PS nanofiber composites can be used as biomedical materials in many fields.

## Declarations

### Author contribution statement

Mayar Mostafa; Nadia G. Kandile; Mahmoud K. Mahmoud; Hassan M. Ibrahim: Conceived and designed the experiments; Performed the experiments; Analyzed and interpreted the data; Contributed reagents, materials, analysis tools or data; Wrote the paper.

### Funding statement

This work was supported by National Research Centre through project ID: E120302.

### Data availability statement

Data included in article/supplementary material/referenced in article.

## Declaration of interests statement

The authors declare no conflict of interest.

## Additional information

Supplementary content related to this article has been published online at <https://doi.org/10.1016/j.heliyon.2022.e08772>.

## Acknowledgements

The authors gratefully acknowledge National Research Centre, for financial support for facilities provided through project ID: E120302.

## References

- [1] S. Huan, L. Bai, G. Liu, W. Cheng, G. Han, Electrospun nanofibrous composites of polystyrene and cellulose nanocrystals: manufacture and characterization, RSC Adv. 5 (63) (2015) 50756–50766.
- [2] S. Priya, A. Murali, D.R. Preeth, K.C. Dharanibalaji, G. Jeyajothi, Green synthesis of silver nanoparticle-embedded poly(methyl methacrylate-co-methacrylic acid) copolymer for fungal-free leathers, Polym. Bull. (2021).
- [3] D. Simões, S.P. Miguel, M.P. Ribeiro, P. Coutinho, A.G. Mendonça, I.J. Correia, Recent advances on antimicrobial wound dressing: a review, Eur. J. Pharm. Biopharm. 127 (2018) 130–141.
- [4] H.M. Li, Q.G. Zhang, N.N. Guo, A.M. Zhu, Q.L. Liu, Ultrafine polystyrene nanofibers and its application in nanofibrous membranes, Chem. Eng. J. 264 (2015) 329–335.
- [5] G. Tao, Y. Wang, R. Cai, H. Chang, K. Song, H. Zuo, et al., Design and performance of sericin/poly(vinyl alcohol) hydrogel as a drug delivery carrier for potential wound dressing application, Mater. Sci. Eng. C 101 (2019) 341–351.
- [6] K.H. Lee, H.Y. Kim, H.J. Bang, Y.H. Jung, S.G. Lee, The change of bead morphology formed on electrospun polystyrene fibers, Polymer 44 (14) (2003) 4029–4034.
- [7] L.W. McKeen, Plastics used in medical devices, in: Handbook of Polymer Applications in Medicine and Medical Devices, Elsevier, 2014, pp. 21–53.
- [8] J.W. Yoon, Y. Park, J. Kim, C.H. Park, Multi-jet electrospinning of polystyrene/polymide 6 blend: thermal and mechanical properties, Fash. Textil. 4 (1) (2017) 9.
- [9] N.N. Patel, M.I. Shekh, K.P. Patel, R.M. Patel, Electrospun Nano Silver Embedded Polystyrene Composite Nanofiber as a Possible Water Disinfectant, 2019.
- [10] T. Uyar, F. Besenbacher, Electrospinning of uniform polystyrene fibers: the effect of solvent conductivity, Polymer 49 (24) (2008) 5336–5343.
- [11] T. Nitanan, P. Opanasopit, P. Akkaramongkolporn, T. Rojanarata, T. Ngawhirunpat, P. Supaphol, Effects of processing parameters on morphology of electrospun polystyrene nanofibers, Kor. J. Chem. Eng. 29 (2) (2012) 173–181.
- [12] E. Yousif, R. Haddad, Photodegradation and photostabilization of polymers, especially polystyrene, SpringerPlus 2 (1) (2013) 1–32.
- [13] R. Sen, B. Zhao, D. Perea, M.E. Itkis, H. Hu, J. Love, et al., Preparation of single-walled carbon nanotube reinforced polystyrene and polyurethane nanofibers and membranes by electrospinning, Nano Lett. 4 (3) (2004) 459–464.
- [14] P. Wang, H. He, R. Cai, G. Tao, M. Yang, H. Zuo, et al., Cross-linking of dialdehyde carboxymethyl cellulose with silk sericin to reinforce sericin film for potential biomedical application, Carbohydr. Polym. 212 (2019) 403–411.
- [15] H.M. Ibrahim, A. Klingner, A review on electrospun polymeric nanofibers: production parameters and potential applications, Polym. Test. (2020) 90.
- [16] H.M. Ibrahim, M.M. Reda, A. Klingner, Preparation and characterization of green carboxymethylchitosan (CMCS) – polyvinyl alcohol (PVA) electrospun nanofibers containing gold nanoparticles (AuNPs) and its potential use as biomaterials, Int. J. Biol. Macromol. 151 (2020) 821–829.
- [17] G. Tao, R. Cai, Y. Wang, H. Zuo, H. He, Fabrication of antibacterial sericin based hydrogel as an injectable and mouldable wound dressing, Mater. Sci. Eng. C 119 (2021) 111597.
- [18] M.M. Bakr, M.A. Taha, H. Osman, H.M. Ibrahim, Novel green printing of cotton, wool and polyester fabrics with natural safflower dye nanoparticles, Egypt. J. Chem. 64 (11) (2021) 6221–6230.
- [19] H.M. Ibrahim, A.A. Aly, G.M. Taha, E.A. El-Alfy, Production of antibacterial cotton fabrics via green treatment with nontoxic natural biopolymer gelatin, Egypt. J. Chem. 63 (2020) 655–696.
- [20] S. Farag, H.M. Ibrahim, A. Amr, M.S. Asker, A. El-Shafai, Preparation and characterization of ion exchanger based on bacterial cellulose for heavy metal cation removal, Egypt. J. Chem. 62 (2019) 457–466.
- [21] B.M. Eid, G.M. El-Sayed, H.M. Ibrahim, N.H. Habib, Durable antibacterial functionality of cotton/polyester blended fabrics using antibiotic/MONPs composite, Fibers Polym. 20 (11) (2019) 2297–2309.
- [22] T. Aysha, M. El-Sedik, S.A. El Megied, H. Ibrahim, Y. Youssef, R. Hrdina, Synthesis, spectral study and application of solid state fluorescent reactive disperse dyes and their antibacterial activity, Arab. J. Chem. 12 (2) (2019) 225–235.
- [23] F.A. Mohamed, H.M. Ibrahim, A.A. Aly, E.A. El-Alfy, Improvement of dyeability and antibacterial properties of gelatin treated cotton fabrics with synthesized reactive dye, Biosci. Res. 15 (4) (2018) 4403–4408.
- [24] S. Huan, G. Liu, G. Han, W. Cheng, Z. Fu, Q. Wu, et al., Effect of experimental parameters on morphological, mechanical and hydrophobic properties of electrospun polystyrene fibers, Materials 8 (5) (2015).

- [25] M. Abrigo, P. Kingshott, S.L. McArthur, Electrospun polystyrene fiber diameter influencing bacterial attachment, proliferation, and growth, *ACS Appl. Mater. Interfaces* 7 (14) (2015) 7644–7652.
- [26] G. Eda, S. Shivkumar, Bead structure variations during electrospinning of polystyrene, *J. Mater. Sci.* 41 (17) (2006) 5704–5708.
- [27] T. Lin, H. Wang, H. Wang, X. Wang, The charge effect of cationic surfactants on the elimination of fibre beads in the electrospinning of polystyrene, *Nanotechnology* 15 (9) (2004) 1375–1381.
- [28] W. Liu, C. Huang, X. Jin, Electrospinning of grooved polystyrene fibers: effect of solvent systems, *Nanoscale Res. Lett.* 10 (1) (2015) 237.
- [29] H.M. Ibrahim, A. Dakrory, A. Klingner, A.M.A. El-Masry, Carboxymethyl chitosan electrospun nanofibers: preparation and its antibacterial activity, *J. Textil. Apparel Technol. Manag.* 9 (2) (2015).
- [30] L. Wannatong, A. Sirivat, P. Supaphol, Effects of solvents on electrospun polymeric fibers: preliminary study on polystyrene, *Polym. Int.* 53 (11) (2004) 1851–1859.
- [31] A.F.M. Seyam, S.M. Hudson, H.M. Ibrahim, A.I. Waly, N.Y. Abou-Zeid, Healing performance of wound dressing from cyanoethyl chitosan electrospun fibres, *Indian J. Fiber Textil Res.* 37 (3) (2012) 205–210.
- [32] H.M. Ibrahim, E.M.R. El-Zairy, Carboxymethylchitosan nanofibers containing silver nanoparticles: preparation, Characterization and Antibacterial activity, *J. Appl. Pharmaceut. Sci.* 6 (7) (2016) 43–48.
- [33] R.M. Mosaad, O.A. Farid, A. Samir, R.M. Mosaad, Preparation of chitosan antioxidant nanoparticles as drug delivery system for enhancing of anti-cancer drug, *Key Eng. Mater.* (2018) 92–97.
- [34] R.M. Mosaad, A. Samir, H.M. Ibrahim, Median lethal dose (LD50) and cytotoxicity of Adriamycin in female albino mice, *J. Appl. Pharmaceut. Sci.* 7 (3) (2017) 77–80.
- [35] F.A. Mohamed, H.M. Ibrahim, M.M. Reda, Eco friendly dyeing of wool and cotton fabrics with reactive dyes (bifunctional) and its antibacterial activity, *Der Pharma Chem.* 8 (16) (2016) 159–167.
- [36] G. Tao, R. Cai, Y. Wang, L. Liu, H. Zuo, P. Zhao, et al., Bioinspired design of AgNPs embedded silk sericin-based sponges for efficiently combating bacteria and promoting wound healing, *Mater. Des.* 180 (2019) 107940.
- [37] L. Liu, R. Cai, Y. Wang, G. Tao, L. Ai, P. Wang, et al., Polydopamine-assisted silver nanoparticle self-assembly on sericin/agar film for potential wound dressing application, *Int. J. Mol. Sci.* 19 (10) (2018).
- [38] A. Kulkarni, V. Bambole, P. Mahanwar, Engineering. Electrospinning of polymers, their modeling and applications, *Polym. Plast. Technol. Eng.* 49 (5) (2010) 427–441.
- [39] R. Sharma, H. Singh, M. Joshi, A. Sharma, T. Garg, A.K. Goyal, et al., Recent advances in polymeric electrospun nanofibers for drug delivery, *Ther. Drug Carrier Syst.* 31 (3) (2014).
- [40] R. Jayakumar, M. Prabaharan, K. Shalumon, K. Chennazhi, S. Nair, Biomedical applications of polymer/silver composite nanofibers, *Biomed. Appl. Polym. Nanofib.* (2011) 263–282.
- [41] H. Ibrahim, M.M. Reda, A. Klingner, Preparation and characterization of green carboxymethylchitosan (CMCS)–Polyvinyl alcohol (PVA) electrospun nanofibers containing gold nanoparticles (AuNPs) and its potential use as biomaterials, *Int. J. Biol. Macromol.* 151 (2020) 821–829.
- [42] R. Thomas, K. Soumya, J. Mathew, E. Radhakrishnan, Electrospun polycaprolactone membrane incorporated with biosynthesized silver nanoparticles as effective wound dressing material, *Appl. Biochem. Biotechnol.* 176 (8) (2015) 2213–2224.
- [43] E. Kowsalya, K. MosaChristas, P. Balashanmugam, J.C. Rani, S. Life, Biocompatible silver nanoparticles/poly (vinyl alcohol) electrospun nanofibers for potential antimicrobial food packaging applications, *Food Packaging and Shelf Life* 21 (2019) 100379.
- [44] A. Uthaman, H.M. Lal, S. Thomas, Characterization, applications. Silver nanoparticle on various synthetic polymer matrices: preparative techniques, characterizations, and applications, *Polym. Nanocomp. Based Silver Nanopart.: Synthesis Charact. Appl.* (2021) 109–138.
- [45] Z. Xu, S. Mahalingam, J. Rohn, G. Ren, M. Edirisinghe, Physio-chemical and antibacterial characteristics of pressure spun nylon nanofibres embedded with functional silver nanoparticles, *Mater. Sci. Eng.* 56 (2015) 195–204.
- [46] B.S. Munteanu, Z. Aytac, G.M. Pricope, T. Uyar, C. Vasile, Poly(lactic acid (PLA)/Silver-NP/VitaminE bionanocomposite electrospun nanofibers with antibacterial and antioxidant activity, *J. Nanoparticle Res.* 16 (10) (2014) 1–12.
- [47] R.G. Nawalakhe, S.M. Hudso, A.M. Seyam, A.I. Waly, N.Y. Abou-Zeid, H.M. Ibrahim, Development of electrospun iminichitosan for improved wound healing application, *J. Eng. Fiber. Fabr.* 7 (2) (2012) 47–55.
- [48] F.A. Mohamed, H.M. Ibrahim, E.A. El-Kharadly, E.A. El-Alfy, Improving dye ability and antimicrobial properties of cotton fabric, *J. Appl. Pharmaceut. Sci.* 6 (2) (2016) 119–123.
- [49] A. Abou-Okeil, H.M. Fahmy, M.M.G. Fouda, A.A. Aly, H.M. Ibrahim, Hyaluronic acid/oxidized K-carrageenan electrospun nanofibers synthesis and antibacterial properties, *BioNanoScience* 11 (3) (2021) 687–695.
- [50] H. He, G. Tao, Y. Wang, R. Cai, P. Guo, L. Chen, et al., In situ green synthesis and characterization of sericin-silver nanoparticle composite with effective antibacterial activity and good biocompatibility, *Mater. Sci. Eng. C* 80 (2017) 509–516.
- [51] Z. Liu, J. Yan, Y.-E. Miao, Y. Huang, T. Liu, Catalytic and antibacterial activities of green-synthesized silver nanoparticles on electrospun polystyrene nanofiber membranes using tea polyphenols, *Compos. B Eng.* 79 (2015) 217–223.
- [52] H.K. Lee, E.H. Jeong, C.K. Baek, J.H. Youk, One-step preparation of ultrafine poly (acrylonitrile) fibers containing silver nanoparticles, *Mater. Lett.* 59 (23) (2005) 2977–2980.
- [53] M.I. Skiba, V.I. Vorobyova, A. Pivovarov, N.P. Makarshenko, Green synthesis of silver nanoparticles in the presence of polysaccharide: optimization and characterization, *J. Nanomater.* (2020) 2020.
- [54] G. Goncalves, P.A. Marques, C.M. Granadeiro, H.I. Nogueira, M. Singh, J. Gracio, Surface modification of graphene nanosheets with gold nanoparticles: the role of oxygen moieties at graphene surface on gold nucleation and growth, *Chem. Mater.* 21 (20) (2009) 4796–4802.
- [55] L.C. Yun'an Qing, R. Li, G. Liu, Y. Zhang, X. Tang, J. Wang, et al., Potential antibacterial mechanism of silver nanoparticles and the optimization of orthopedic implants by advanced modification technologies, *Int. J. Nanomed.* 13 (2018) 3311.
- [56] A.G. Hassabo, A.A. Nada, H.M. Ibrahim, N.Y. Abou-Zeid, Impregnation of silver nanoparticles into polysaccharide substrates and their properties, *Carbohydr. Polym.* 122 (2015) 343–350.
- [57] T.C. Dakal, A. Kumar, R.S. Majumdar, V. Yadav, Mechanistic basis of antimicrobial actions of silver nanoparticles, *Front. Microbiol.* 7 (2016) 1831.
- [58] S. Rahman, L. Rahman, A.T. Khalil, N. Ali, D. Zia, M. Ali, et al., Endophyte-mediated synthesis of silver nanoparticles and their biological applications, *Appl. Microbiol. Biotechnol.* 103 (6) (2019) 2551–2569.